



---

*Research article*

## Analytical results for positivity of discrete fractional operators with approximation of the domain of solutions

Pshtiwan Othman Mohammed<sup>1,\*</sup>, Donal O'Regan<sup>2</sup>, Dumitru Baleanu<sup>3,4,5,\*</sup>, Y. S. Hamed<sup>6</sup> and Ehab E. Elattar<sup>7</sup>

<sup>1</sup> Department of Mathematics, College of Education, University of Sulaimani, Sulaimani 46001, Kurdistan Region, Iraq

<sup>2</sup> School of Mathematical and Statistical Sciences, National University of Ireland, Galway, Ireland

<sup>3</sup> Department of Mathematics, Cankaya University, Balgat 06530, Ankara, Turkey

<sup>4</sup> Institute of Space Sciences, R76900 Magurele-Bucharest, Romania

<sup>5</sup> China Medical University Hospital, China Medical University, Taichung 40402, Taiwan

<sup>6</sup> Department of Mathematics and Statistics, College of Science, Taif University, Taif 21944, Saudi Arabia

<sup>7</sup> Department of Electrical Engineering, College of Engineering, Taif University, Taif 21944, Saudi Arabia

\* **Correspondence:** Email: pshtiwansangawi@gmail.com, dumitru@cankaya.edu.tr.

**Abstract:** We study the monotonicity method to analyse nabla positivity for discrete fractional operators of Riemann-Liouville type based on exponential kernels, where  $\left({}^{CFR}_{c_0}\nabla^\theta F\right)(t) > -\epsilon \Lambda(\theta - 1)(\nabla F)(c_0 + 1)$  such that  $(\nabla F)(c_0 + 1) \geq 0$  and  $\epsilon > 0$ . Next, the positivity of the fully discrete fractional operator is analyzed, and the region of the solution is presented. Further, we consider numerical simulations to validate our theory. Finally, the region of the solution and the cardinality of the region are discussed via standard plots and heat map plots. The figures confirm the region of solutions for specific values of  $\epsilon$  and  $\theta$ .

**Keywords:** discrete fractional calculus; Caputo-Fabrizio fractional difference; nabla positivity; numerical analysis

---

### 1. Introduction

The construction of discrete fractional sums and differences from the knowledge of samples of their corresponding continuous integrals and derivatives arises in the context of discrete fractional calculus;

see [1–6] for more details. Recently, discrete fractional operators with more general forms of their kernels and properties have gathered attention in both areas of physics and mathematics; see [7–10].

In discrete fractional calculus theory, we say that  $F$  is monotonically increasing at a time step  $t$  if the nabla of  $F$  is non-negative, i.e.,  $(\nabla F)(t) := F(t) - F(t - 1) \geq 0$  for each  $t$  in the time scale set  $\mathbb{N}_{c_0+1} := \{c_0 + 1, c_0 + 2, \dots\}$ . Moreover, the function  $F$  is  $\theta$ -monotonically increasing (or decreasing) on  $\mathbb{N}_{c_0}$  if  $F(t + 1) > \theta F(t)$  (or  $F(t + 1) < \theta F(t)$ ) for each  $t \in \mathbb{N}_a$ . In [11, 12] the authors considered 1-monotonicity analysis for standard discrete Riemann-Liouville fractional differences defined on  $\mathbb{N}_0$  and in [13] the authors generalized the above by introducing  $\theta$ -monotonicity increasing and decreasing functions and then obtained some  $\theta$ -monotonicity analysis results for discrete Riemann-Liouville fractional differences defined on  $\mathbb{N}_0$ . In [14–16], the authors considered monotonicity and positivity analysis for discrete Caputo, Caputo-Fabrizio and Attangana-Baleanu fractional differences and in [17, 18] the authors considered monotonicity and positivity results for abstract convolution equations that could be specialized to yield new insights into qualitative properties of fractional difference operators. In [19], the authors presented positivity and monotonicity results for discrete Caputo-Fabrizio fractional operators which cover both the sequential and non-sequential cases, and showed both similarities and dissimilarities between the exponential kernel case (that is included in Caputo-Fabrizio fractional operators) and fractional differences with other types of kernels. Also in [20] the authors extended the results in [19] to discrete Attangana-Baleanu fractional differences with Mittag-Leffler kernels. The main theoretical developments of monotonicity and positivity analysis in discrete fractional calculus can be found in [21–24] for nabla differences, and in [25–28] for delta differences.

The main idea in this article is to analyse discrete Caputo-Fabrizio fractional differences with exponential kernels in the Riemann-Liouville sense. The results are based on a notable lemma combined with summation techniques. The purpose of this article is two-fold. First we show the positiveness of discrete fractional operators from a theoretical point of view. Second we shall complement the theoretical results numerically and graphically based on the standard plots and heat map plots.

The plan of the article is as follows. In Section 2 we present discrete fractional operators and the main lemma. Section 3 analyses the discrete fractional operator in a theoretical sense. In Section 4 we discuss our theoretical strategy on standard plots (Subsection 4.1) and heat map plots (Subsection 4.2). Finally, in Section 5 we summarize our findings.

## 2. Basic definitions and a lemma

First we recall the definitions in discrete fractional calculus; see [2, 3, 5] for more information.

**Definition 2.1** (see [2, Definition 2.24]). Let  $c_0 \in \mathbb{R}$ ,  $0 < \theta \leq 1$ ,  $F$  be defined on  $\mathbb{N}_{c_0}$  and  $\Lambda(\theta) > 0$  be a normalization constant. Then the following operator

$$\left({}^{CFR}_{c_0} \nabla^\theta F\right)(t) := \Lambda(\theta) \nabla_t \sum_{r=c_0+1}^t F(r)(1-\theta)^{t-r} \quad \{t \in \mathbb{N}_{c_0+1}\},$$

is called the discrete Caputo-Fabrizio fractional operator with exponential kernels in the Riemann-

Liouville sense  $CF_R$ , and the following operator

$$\left({}^{CF_C} \nabla^\theta \mathbf{F}\right)(t) := \Lambda(\theta) \sum_{r=c_0+1}^t (\nabla_r \mathbf{F})(r)(1-\theta)^{t-r} \quad \{t \in \mathbb{N}_{c_0+1}\},$$

is called the discrete Caputo-Fabrizio fractional operator with exponential kernels in the Caputo sense  $CF_C$ .

**Definition 2.2** (see [3]). For  $\mathbf{F} : \mathbb{N}_{c_0-\kappa} \rightarrow \mathbb{R}$  with  $\kappa < \theta \leq \kappa + 1$  and  $\kappa \in \mathbb{N}_0$ , the discrete nabla  $CF_C$  and  $CF_R$  fractional differences can be expressed as follows:

$$\left({}^{CF_C} \nabla^\theta \mathbf{F}\right)(t) = \left({}^{CF_C} \nabla^{\theta-\kappa} \nabla^\kappa \mathbf{F}\right)(t),$$

and

$$\left({}^{CF_R} \nabla^\theta \mathbf{F}\right)(t) = \left({}^{CF_R} \nabla^{\theta-\kappa} \nabla^\kappa \mathbf{F}\right)(t),$$

respectively, for each  $t \in \mathbb{N}_{c_0+1}$ .

The following lemma is essential later.

**Lemma 2.1.** Assume that  $\mathbf{F}$  is defined on  $\mathbb{N}_{c_0}$  and  $1 < \theta < 2$ . Then the  $CF_R$  fractional difference is

$$\begin{aligned} \left({}^{CF_R} \nabla^\theta \mathbf{F}\right)(t) = \Lambda(\theta - 1) & \left\{ (\nabla \mathbf{F})(t) + (1 - \theta)(2 - \theta)^{t-c_0-2} (\nabla \mathbf{F})(c_0 + 1) \right. \\ & \left. + (1 - \theta) \sum_{r=c_0+2}^{t-1} (\nabla_r \mathbf{F})(r)(2 - \theta)^{t-r-1} \right\}, \end{aligned}$$

for each  $t \in \mathbb{N}_{c_0+2}$ .

*Proof.* From Definitions 2.1 and 2.2, the following can be deduced for  $1 < \theta < 2$  :

$$\begin{aligned} \left({}^{CF_R} \nabla^\theta \mathbf{F}\right)(t) &= \Lambda(\theta - 1) \left\{ \sum_{r=c_0+1}^t (\nabla_r \mathbf{F})(r)(2 - \theta)^{t-r} - \sum_{r=c_0+1}^{t-1} (\nabla_r \mathbf{F})(r)(2 - \theta)^{t-r-1} \right\} \\ &= \Lambda(\theta - 1) \left\{ (\nabla \mathbf{F})(t) + \sum_{r=c_0+1}^{t-1} (\nabla_r \mathbf{F})(r) \left[ (2 - \theta)^{t-r} - (2 - \theta)^{t-r-1} \right] \right\} \\ &= \Lambda(\theta - 1) \left\{ (\nabla \mathbf{F})(t) + (1 - \theta)(2 - \theta)^{t-c_0-2} (\nabla \mathbf{F})(c_0 + 1) \right. \\ & \quad \left. + (1 - \theta) \sum_{r=c_0+2}^{t-1} (\nabla_r \mathbf{F})(r)(2 - \theta)^{t-r-1} \right\}, \end{aligned}$$

for each  $t \in \mathbb{N}_{c_0+2}$ .

### 3. Theoretical analysis results

In the following theorem, we will show that  $F$  is monotonically increasing at two time steps even if  $({}^{CFR}_{c_0}\nabla^\theta F)(t)$  is negative at the two time steps.

**Theorem 3.1.** *Let the function  $F$  be defined on  $\mathbb{N}_{c_0+1}$ , and let  $1 < \theta < 2$  and  $\epsilon > 0$ . Assume that*

$$({}^{CFR}_{c_0}\nabla^\theta F)(t) > -\epsilon \Lambda(\theta - 1)(\nabla F)(c_0 + 1) \quad \text{for } t \in \{c_0 + 2, c_0 + 3\} \quad \text{s.t.} \quad (\nabla F)(c_0 + 1) \geq 0. \quad (3.1)$$

*If  $(1 - \theta)(2 - \theta) < -\epsilon$ , then  $(\nabla F)(c_0 + 2)$  and  $(\nabla F)(c_0 + 3)$  are both nonnegative.*

*Proof.* From Lemma 2.1 and condition (3.1) we have

$$(\nabla F)(t) \geq -(\nabla F)(c_0 + 1)[(1 - \theta)(2 - \theta)^{t-c_0-2} + \epsilon] - (1 - \theta) \sum_{r=c_0+2}^{t-1} (\nabla_r F)(r)(2 - \theta)^{t-r-1}, \quad (3.2)$$

for each  $t \in \mathbb{N}_{c_0+2}$ . At  $t = c_0 + 2$ , we have

$$\begin{aligned} (\nabla F)(c_0 + 2) &\geq -(\nabla F)(c_0 + 1)[(1 - \theta) + \epsilon] - (1 - \theta) \underbrace{\sum_{r=c_0+2}^{c_0+1} (\nabla_r F)(r)(2 - \theta)^{c_0+1-r}}_{=0} \\ &\geq 0, \end{aligned}$$

where we have used  $(1 - \theta) < (1 - \theta)(2 - \theta) < -\epsilon$  and  $(\nabla F)(c_0 + 1) \geq 0$  by assumption. At  $t = c_0 + 3$ , it follows from (3.2) that

$$\begin{aligned} (\nabla F)(c_0 + 3) &= -(\nabla F)(c_0 + 1)[(1 - \theta)(2 - \theta) + \epsilon] - (1 - \theta) \sum_{r=c_0+2}^{c_0+2} (\nabla_r F)(r)(2 - \theta)^{c_0+2-r} \\ &= -\underbrace{(\nabla F)(c_0 + 1)}_{\geq 0} \underbrace{[(1 - \theta)(2 - \theta) + \epsilon]}_{< 0} - \underbrace{(1 - \theta)}_{< 0} \underbrace{(\nabla F)(c_0 + 2)}_{\geq 0} \geq 0, \quad (3.3) \end{aligned}$$

as required. Hence the proof is completed.

**Remark 3.1.** *It worth mentioning that Figure 1 shows the graph of  $\theta \mapsto (1 - \theta)(2 - \theta)$  for  $\theta \in (1, 2)$ .*

In order for Theorem 3.1 to be applicable, the allowable range of  $\epsilon$  is  $\epsilon \in (0, -(2 - \theta)(1 - \theta))$  for a fixed  $\theta \in (1, 2)$

Now, we can define the set  $\mathcal{H}_{\kappa, \epsilon}$  as follows

$$\mathcal{H}_{\kappa, \epsilon} := \left\{ \theta \in (1, 2) : (1 - \theta)(2 - \theta)^{\kappa - c_0 - 2} < -\epsilon \right\} \subseteq (1, 2), \quad \forall \kappa \in \mathbb{N}_{c_0+3}.$$

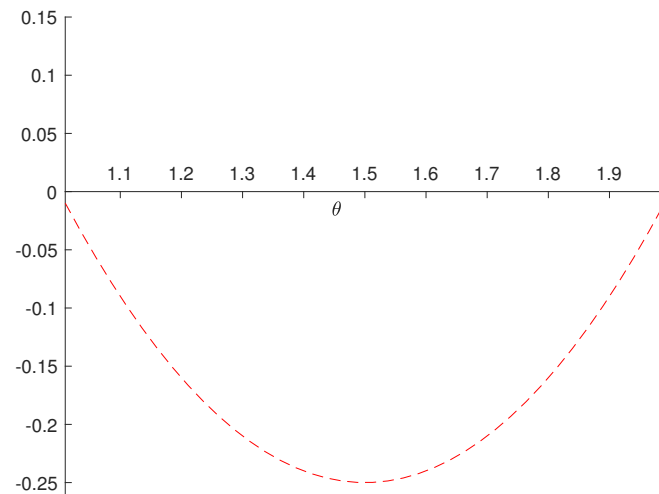


**Figure 1.** Graph of  $\theta \mapsto (1 - \theta)(2 - \theta)$  for  $\theta \in (1, 2)$ .

The following lemma shows that the collection  $\{\mathcal{H}_{\kappa, \epsilon}\}_{\kappa=c_0+1}^{\infty}$  forms a nested collection of decreasing sets for each  $\epsilon > 0$ .

**Lemma 3.1.** *Let  $1 < \theta < 2$ . Then, for each  $\epsilon > 0$  and  $\kappa \in \mathbb{N}_{c_0+3}$  we have that  $\mathcal{H}_{\kappa+1, \epsilon} \subseteq \mathcal{H}_{\kappa, \epsilon}$ .*

*Proof.* Let  $\theta \in \mathcal{H}_{\kappa+1, \epsilon}$  for some fixed but arbitrary  $\kappa \in \mathbb{N}_{c_0+3}$  and  $\epsilon > 0$ . Then we have

$$(1 - \theta)(2 - \theta)^{\kappa - c_0 - 1} = (1 - \theta)(2 - \theta)(2 - \theta)^{\kappa - c_0 - 2} < -\epsilon.$$

Considering  $1 < \theta < 2$  and  $\kappa \in \mathbb{N}_{c_0+3}$ , we have  $0 < 2 - \theta < 1$ . Consequently, we have

$$(1 - \theta)(2 - \theta)^{\kappa - c_0 - 2} < -\epsilon \cdot \underbrace{\frac{1}{2 - \theta}}_{>1} < -\epsilon.$$

This implies that  $\theta \in \mathcal{H}_{\kappa, \epsilon}$ , and thus  $\mathcal{H}_{\kappa+1, \epsilon} \subseteq \mathcal{H}_{\kappa, \epsilon}$ .

Now, Theorem 3.1 and Lemma 3.1 lead to the following corollary.

**Corollary 3.1.** *Let  $F$  be a function defined on  $\mathbb{N}_{c_0+1}$ ,  $\theta \in (1, 2)$  and*

$$\left( {}^{CFR}_{c_0} \nabla^{\theta} F \right) (t) > -\epsilon \Lambda(\theta - 1) (\nabla F)(c_0 + 1) \quad \text{such that} \quad (\nabla F)(c_0 + 1) \geq 0, \quad (3.4)$$

for each  $t \in \mathbb{N}_{c_0+3}^s := \{c_0 + 3, c_0 + 4, \dots, s\}$  and some  $s \in \mathbb{N}_{c_0+3}$ . If  $\theta \in \mathcal{H}_{s, \epsilon}$ , then we have  $(\nabla F)(t) \geq 0$  for each  $t \in \mathbb{N}_{c_0+1}^s$ .

*Proof.* From the assumption  $\theta \in \mathcal{H}_{s, \epsilon}$  and Lemma 3.1, we have

$$\theta \in \mathcal{H}_{s, \epsilon} = \mathcal{H}_{s, \epsilon} \cap \bigcap_{\kappa=c_0+3}^{s-1} \mathcal{H}_{\kappa, \epsilon}.$$

This leads to

$$(1 - \theta)(2 - \theta)^{t-c_0-2} < -\epsilon, \quad (3.5)$$

for each  $t \in \mathbb{N}_{c_0+3}^s$ .

Now we use the induction process. First for  $t = c_0 + 3$  we obtain  $(\nabla F)(c_0 + 3) \geq 0$  directly as in Theorem 3.1 by considering inequalities (Eq 3.4) and (Eq 3.5) together with the given assumption  $(\nabla F)(c_0 + 1) \geq 0$ . As a result, we can inductively iterate inequality (Eq 3.2) to get

$$(\nabla F)(t) \geq 0,$$

for each  $t \in \mathbb{N}_{c_0+2}^s$ . Moreover,  $(\nabla F)(c_0 + 1) \geq 0$  by assumption. Thus,  $(\nabla F)(t) \geq 0$  for each  $t \in \mathbb{N}_{c_0+1}^s$  as desired.

#### 4. Numerical analysis results

In this section, we consider the methodology for the positivity of  $\nabla F$  based on previous observations in Theorem 3.1 and Corollary 3.1 in such a way that the initial conditions are known. Later, we will illustrate other parts of our article via standard plots and heat maps for different values of  $\theta$  and  $\epsilon$ . The computations in this section were performed with MATLAB software.

**Example 4.1.** Considering Lemma 2.1 with  $t := c_0 + 3$ :

$$\begin{aligned} \left( {}^{CF_R}_{c_0} \nabla^\theta F \right) (c_0 + 3) &= \Lambda(\theta - 1) \left\{ (\nabla F)(c_0 + 3) + (1 - \theta)(2 - \theta)(\nabla F)(c_0 + 1) \right. \\ &\quad \left. + (1 - \theta) \sum_{r=c_0+2}^{c_0+2} (\nabla_r F)(r)(2 - \theta)^{c_0+2-r} \right\}. \end{aligned}$$

For  $c_0 = 0$ , it follows that

$$\begin{aligned} \left( {}^{CF_R}_0 \nabla^\theta F \right) (3) &= \Lambda(\theta - 1) \left\{ (\nabla F)(3) + (1 - \theta)(2 - \theta)(\nabla F)(1) + (1 - \theta) \sum_{r=2}^2 (\nabla_r F)(r)(2 - \theta)^{2-r} \right\} \\ &= \Lambda(\theta - 1) \left\{ (\nabla F)(3) + (1 - \theta)(2 - \theta)(\nabla F)(1) + (1 - \theta)(\nabla F)(2) \right\} \\ &= \Lambda(\theta - 1) \left\{ F(3) - F(2) + (1 - \theta)(2 - \theta)[F(1) - F(0)] + (1 - \theta)[F(2) - F(1)] \right\}. \end{aligned}$$

If we take  $\theta = 1.99$ ,  $F(0) = 0$ ,  $F(1) = 1$ ,  $F(2) = 1.001$ ,  $F(3) = 1.005$ , and  $\epsilon = 0.007$ , we have

$$\begin{aligned} \left( {}^{CF_R}_0 \nabla^{1.99} F \right) (3) &= \Lambda(0.99) \left\{ 0.004 + (-0.99)(0.01)(0) + (-0.99)(0.001) \right\} \\ &= -0.0069 \Lambda(0.99) > -0.007 \Lambda(0.99) = -\epsilon \Lambda(0.99) (\nabla F)(1). \end{aligned}$$

In addition, we see that  $(1 - \theta)(2 - \theta) = -0.0099 < -0.007 = -\epsilon$ . Since the required conditions are satisfied, Theorem 3.1 ensures that  $(\nabla F)(3) > 0$ .

#### 4.1. Standard plots

In Figure 2, the sets  $\mathcal{H}_{\kappa,0.008}$  and  $\mathcal{H}_{\kappa,0.004}$  are shown for different values of  $\kappa$ , respectively in Figure 2a,b. It is noted that  $\mathcal{H}_{\kappa,0.008}$  and  $\mathcal{H}_{\kappa,0.004}$  decrease by increasing the values of  $\kappa$ . Moreover, in Figure 2a, the set  $\mathcal{H}_{\kappa,0.008}$  becomes empty for  $\kappa \geq 45$ ; however, in Figure 2b, we observe the non-emptiness of the set  $\mathcal{H}_{\kappa,0.004}$  for many larger values of  $\kappa$  up to 90. We think that the measures of  $\mathcal{H}_{\kappa,0.008}$  and  $\mathcal{H}_{\kappa,0.004}$  are not symmetrically distributed when  $\kappa$  increases (see Figure 2a,b). We do not have a good conceptual explanation for why this symmetric behavior is observed. In fact, it is not clear why the discrete nabla fractional difference  ${}^{CFR}_{c_0}\nabla^\theta$  seems to give monotonically when  $\theta \rightarrow 1$  rather than for  $\theta \rightarrow 2$ , specifically, it gives a maximal information when  $\theta$  is very close to 1 as  $\epsilon \rightarrow 0^+$ .

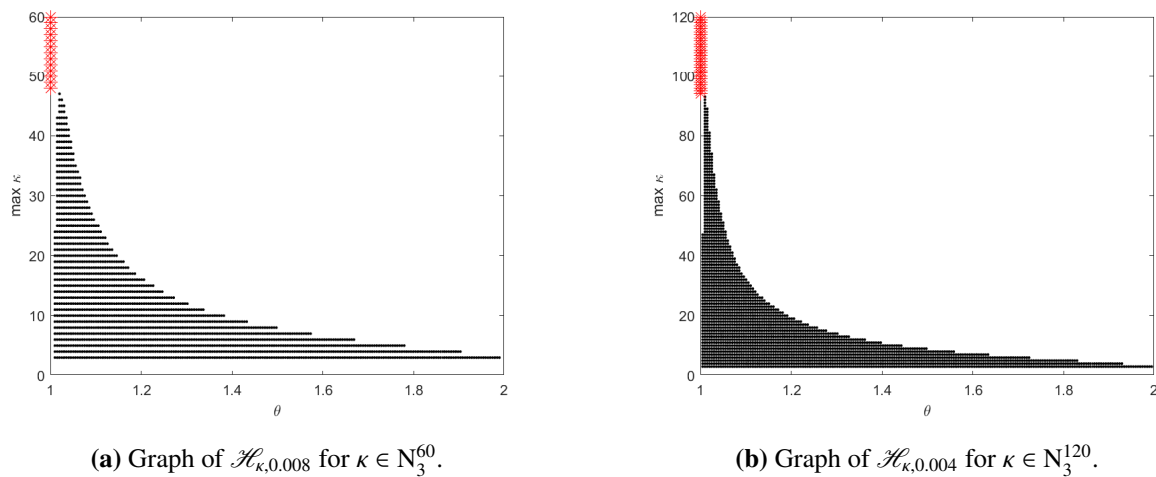


**Figure 2.** Graph of  $\mathcal{H}_{\kappa,\epsilon}$  for different values of  $\kappa$  and  $\epsilon$ .

In the next figure (Figure 3), we have chosen a smaller  $\epsilon$  ( $\epsilon = 0.001$ ), we see that the set  $\mathcal{H}_{\kappa,0.001}$  is non-empty for  $\kappa > 320$ . This tells us that small choices in  $\epsilon$  give us a more widely applicable result.

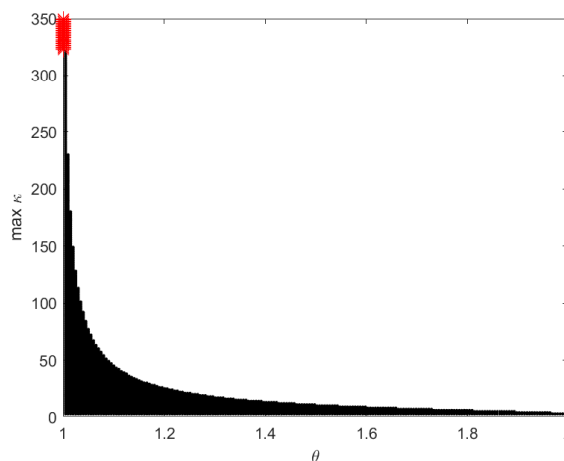


**Figure 3.** Graph of  $\mathcal{H}_{\kappa,\epsilon}$  for  $\kappa \in \mathbb{N}_3^{350}$  and  $\epsilon = 0.001$ .

## 4.2. Heat map plots

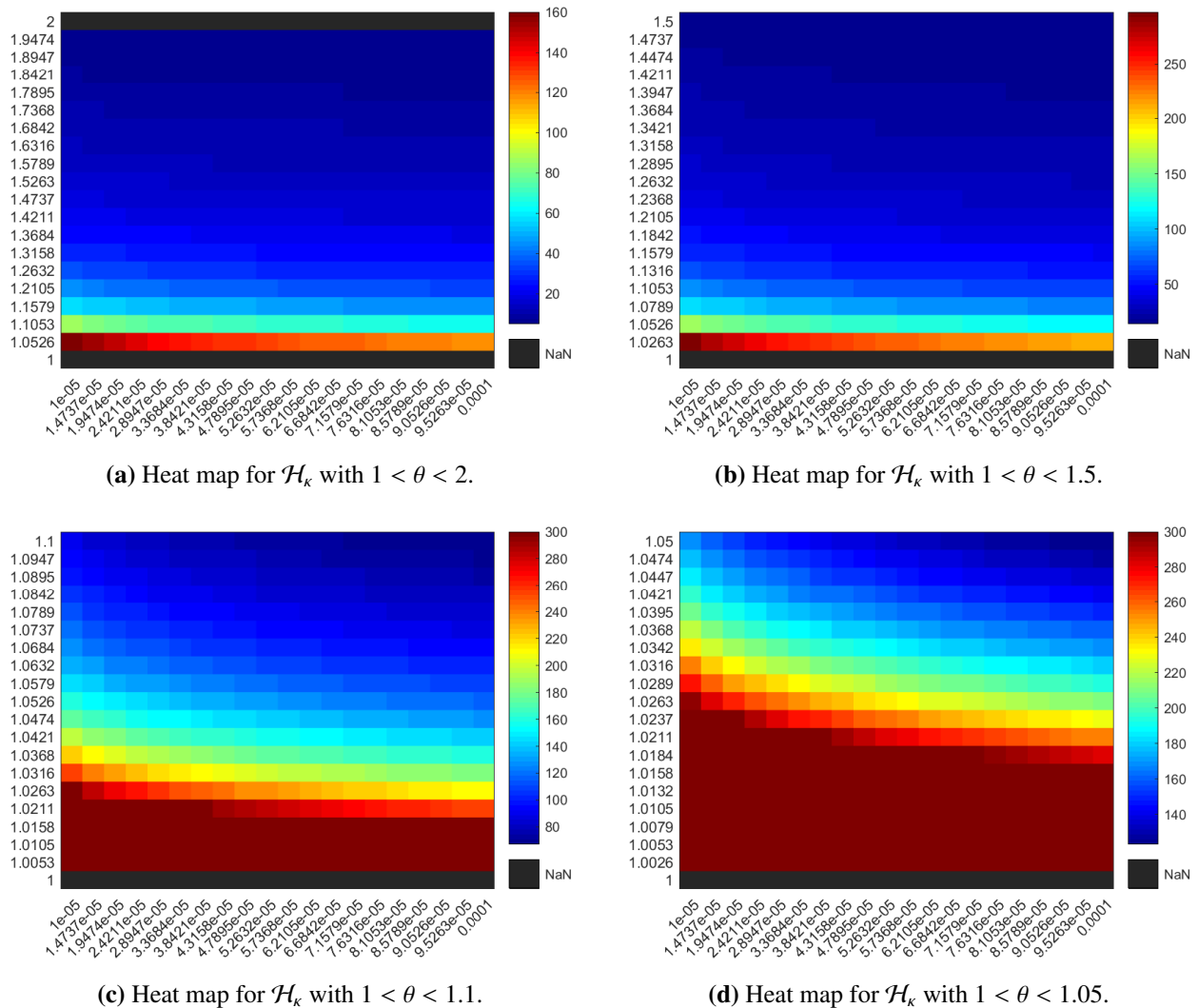


**Figure 4.** The cardinality of  $\mathcal{H}_k$  for different values of  $\theta$  with  $0.00001 \leq \epsilon \leq 0.0001$  in heat maps.

In this part, we introduce the set  $\mathcal{H}_k := \{K : \theta \in \mathcal{H}_{k,\epsilon}\}$  to simulate our main theoretical findings for the cardinality of the set  $\mathcal{H}_k$  via heat maps in Figure 4a–d. In these figures: we mean the warm colors such as red ones and the cool colors such as blue ones. Moreover, the  $\theta$  values are on the  $x$ -axis and  $\epsilon$  values are on the  $y$ -axis. We choose  $\epsilon$  in the interval  $[0.00001, 0.0001]$ . Then, the conclusion of these figures are as follows:

- In Figure 4a when  $\theta \in (1, 2)$  and Figure 4b when  $\theta \in (1, 1.5)$ , we observe that the warmer colors are somewhat skewed toward  $\theta$  very close to 1, and the cooler colors cover the rest of the figures for  $\theta$  above 1.05.
- In Figure 4c,d, the warmest colors move strongly towards the lower values of  $\theta$ , especially, when  $\theta \in (1, 1.05)$ . Furthermore, when as  $\theta$  increases to up to 1.0368, it drops sharply from magenta



to cyan, which implies a sharp decrease in the cardinality of  $\mathcal{H}_\kappa$  for a small values of  $\epsilon$  as in the interval  $[0.00001, 0.0001]$ .

On the other hand, for larger values of  $\epsilon$ , the set  $\mathcal{H}_\kappa$  will tend to be empty even if we select a smaller  $\theta$  in such an interval  $(1, 1.05)$ . See the following Figure 5a,b for more.

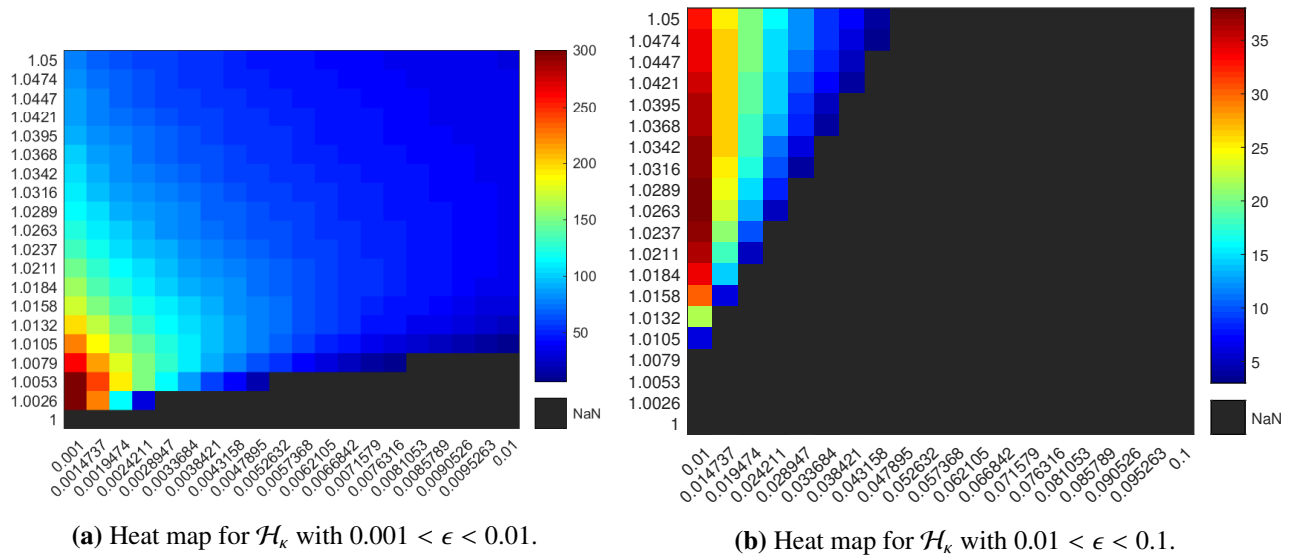


**Figure 5.** The cardinality of  $\mathcal{H}_\kappa$  for different values of  $\epsilon$  with  $1 < \theta < 1.05$  in heat maps.

In conclusion, from Figures 4 and 5, we see that: For a smaller value of  $\epsilon$ , the set  $\mathcal{H}_{\kappa,\epsilon}$  tends to remain non-empty (see Figure 4), unlike for a larger value of  $\epsilon$  (see Figure 5). Furthermore, these verify that Corollary 3.1 will be more applicable for  $1 < \theta < 1.05$  and  $0.01 < \epsilon < 0.1$  as shown in Figure 4d.

Although, our numerical data strongly note the sensitivity of the set  $\mathcal{H}_\kappa$  when slight increasing in  $\epsilon$  is observed for  $\theta$  close to 2 compares with  $\theta$  close to 1.

## 5. Concluding remarks

In this paper we developed a positivity method for analysing discrete fractional operators of Riemann-Liouville type based on exponential kernels. In our work we have found that  $(\nabla F)(3) \geq 0$  when  $({}^{CFR}_{c_0} \nabla^\theta F)(t) > -\epsilon \Lambda(\theta - 1)(\nabla F)(c_0 + 1)$  such that  $(\nabla F)(c_0 + 1) \geq 0$  and  $\epsilon > 0$ . We continue to extend this result for each value of  $t$  in  $\mathbb{N}_{c_0+1}^s$  as we have done in Corollary 3.1.

In addition we presented standard plots and heat map plots for the discrete problem that is solved numerically. Two of the graphs are standard plots for  $\mathcal{H}_{\kappa,\epsilon}$  for different values of  $\kappa$  and  $\epsilon$  (see Figure 2), and the other six graphs consider the cardinality of  $\mathcal{H}_\kappa$  for different values of  $\epsilon$  and  $\theta$  (see Figures 4 and 5). These graphs ensure the validity of our theoretical results.

In the future we hope to apply our method to other types of discrete fractional operators which include Mittag-Leffler and their extensions in kernels; see for example [5, 6].

## Acknowledgements

This work was supported by the Taif University Researchers Supporting Project Number (TURSP-2020/86), Taif University, Taif, Saudi Arabia.

## Conflict of interest

The authors declare there is no conflict of interest.

## References

1. C. Goodrich, A. C. Peterson, *Discrete Fractional Calculus*, Springer, Berlin, 2015. <https://doi.org/10.1007/978-3-319-25562-0>
2. T. Abdeljawad, D. Baleanu, On fractional derivatives with exponential kernel and their discrete versions, *Rep. Math. Phys.*, **80** (2017), 11–27. [https://doi.org/10.1016/S0034-4877\(17\)30059-9](https://doi.org/10.1016/S0034-4877(17)30059-9)
3. T. Abdeljawad, Q. M. Al-Mdallal, M. A. Hajji, Arbitrary order fractional difference operators with discrete exponential kernels and applications, *Discrete Dyn. Nat. Soc.*, **2017** (2017). <https://doi.org/10.1155/2017/4149320>
4. T. Abdeljawad, On Riemann and Caputo fractional differences, *Comput. Math. Appl.*, **62** (2011), 1602–1611. <https://doi.org/10.1016/j.camwa.2011.03.036>
5. T. Abdeljawad, Different type kernel  $h$ -fractional differences and their fractional  $h$ -sums, *Chaos, Solitons Fractals*, **116** (2018), 146–156. <https://doi.org/10.1016/j.chaos.2018.09.022>
6. P. O. Mohammed, T. Abdeljawad, Discrete generalized fractional operators defined using  $h$ -discrete Mittag-Leffler kernels and applications to AB fractional difference systems, *Math. Methods Appl. Sci.*, (2020), 1–26, <https://doi.org/10.1002/mma.7083>
7. G. C. Wu, M. K. Luo, L. L. Huang, S. Banerjee, Short memory fractional differential equations for new neural network and memristor design, *Nonlinear Dyn.*, **100** (2020), 3611–3623. <https://doi.org/10.1007/s11071-020-05572-z>
8. L. L. Huang, G. C. Wu, D. Baleanu, H. Y. Wang, Discrete fractional calculus for interval-valued systems, *Fuzzy Sets Syst.*, **404** (2021), 141–158. <https://doi.org/10.1016/j.fss.2020.04.008>
9. T. Abdeljawad, S. Banerjee, G. C. Wu, Discrete tempered fractional calculus for new chaotic systems with short memory and image encryption, *Optik*, **2018** (2020), 163698. <https://doi.org/10.1016/j.ijleo.2019.163698>
10. G. C. Wu, D. Baleanu, Discrete fractional logistic map and its chaos, *Nonlinear Dyn.*, **75** (2014), 283–287. <https://doi.org/10.1007/s11071-013-1065-7>
11. R. Dahal, C. S. Goodrich, A monotonicity result for discrete fractional difference operators, *Arch. Math.*, **102** (2014), 293–299. <https://doi.org/10.1007/s00013-014-0620-x>
12. C. S. Goodrich, A convexity result for fractional differences, *Appl. Math. Lett.*, **35** (2014), 158–162. <https://doi.org/10.1016/j.aml.2014.04.013>
13. F. Atici, M. Uyanik, Analysis of discrete fractional operators, *Appl. Anal. Discrete Math.*, **9** (2015), 139–149. <https://doi.org/10.2298/AADM150218007A>

14. P. O. Mohammed, O. Almutairi, R. P. Agarwal, Y. S. Hamed, On convexity, monotonicity and positivity analysis for discrete fractional operators defined using exponential kernels, *Fractal Fractional*, **6** (2022), 55. <https://doi.org/10.3390/fractalfract6020055>
15. T. Abdeljawad, D. Baleanu, Monotonicity analysis of a nabla discrete fractional operator with discrete Mittag-Leffler kernel, *Chaos, Solitons Fractals*, **102** (2017), 106–110. <https://doi.org/10.1016/j.chaos.2017.04.006>
16. P. O. Mohammed, C. S. Goodrich, A. B. Brzo, Y. S. Hamed, New classifications of monotonicity investigation for discrete operators with Mittag-Leffler kernel, *Math. Biosci. Eng.*, **19** (2022), 4062–4074. <https://doi.org/10.3934/mbe.2022186>
17. C. Goodrich, C. Lizama, Positivity, monotonicity, and convexity for convolution operators, *Discrete Contin. Dyn. Syst.*, **40** (2020), 4961–4983. <https://doi.org/10.3934/dcds.2020207>
18. C. S. Goodrich, B. Lyons, Positivity and monotonicity results for triple sequential fractional differences via convolution, *Analysis*, **40** (2020), 89–103. <https://doi.org/10.1515/anly-2019-0050>
19. C. S. Goodrich, J. M. Jonnalagadda, B. Lyons, Convexity, monotonicity and positivity results for sequential fractional nabla difference operators with discrete exponential kernels, *Math. Methods Appl. Sci.*, **44** (2021), 7099–7120. <https://doi.org/10.1002/mma.7247>
20. P. O. Mohammed, C. S. Goodrich, F. K. Hamasalh, A. Kashuri, Y. S. Hamed, On positivity and monotonicity analysis for discrete fractional operators with discrete Mittag-Leffler kernel, *Math. Methods Appl. Sci.*, (2022), 1–20. <https://doi.org/10.1002/mma.8176>
21. B. Jia, L. Erbe, A. Peterson, Two monotonicity results for nabla and delta fractional differences, *Arch. Math.*, **104** (2015), 589–597. <https://doi.org/10.1007/s00013-015-0765-2>
22. R. Dahal, C. S. Goodrich, Mixed order monotonicity results for sequential fractional nabla differences, *J. Differ. Equations Appl.*, **25** (2019), 837–854. <https://doi.org/10.1080/10236198.2018.1561883>
23. I. Suwan, T. Abdeljawad, F. Jarad, Monotonicity analysis for nabla  $h$ -discrete fractional Atangana-Baleanu differences, *Chaos, Solitons Fractals*, **117** (2018), 50–59. <https://doi.org/10.1016/j.chaos.2018.10.010>
24. F. Du, B. Jia, L. Erbe, A. Peterson, Monotonicity and convexity for nabla fractional  $(q, h)$ -differences, *J. Differ. Equations Appl.*, **22** (2016), 1224–1243. <https://doi.org/10.1080/10236198.2016.1188089>
25. P. O. Mohammed, T. Abdeljawad, F. K. Hamasalh, On Riemann-Liouville and Caputo fractional forward difference monotonicity analysis, *Mathematics*, **9** (2021), 1303. <https://doi.org/10.3390/math9111303>
26. R. Dahal, C. S. Goodrich, B. Lyons, Monotonicity results for sequential fractional differences of mixed orders with negative lower bound, *J. Differ. Equations Appl.*, **27** (2021), 1574–1593. <https://doi.org/10.1080/10236198.2021.1999434>
27. C. S. Goodrich, A note on convexity, concavity, and growth conditions in discrete fractional calculus with delta difference, *Math. Inequal. Appl.*, **19** (2016), 769–779. <https://doi.org/10.7153/mia-19-57>

- 
28. C. S. Goodrich, A sharp convexity result for sequential fractional delta differences, *J. Differ. Equations Appl.*, **23** (2017), 1986–2003. <https://doi.org/10.1080/10236198.2017.1380635>



AIMS Press

©2022 the Author(s), licensee AIMS Press. This is an open access article distributed under the terms of the Creative Commons Attribution License (<http://creativecommons.org/licenses/by/4.0>)